Inorg. Chem. **2004**, *43*, 4994–5002

Excited-State Dynamics of *fac*-[Re^{I}(L)(CO)$_3$(phen)]$^+$ and *fac*-[Re^{I}(L)(CO)$_3$(5-NO$_2$-phen)]$^+$ (L = Imidazole, 4-Ethylpyridine; Phen = 1,10-Phenanthroline) Complexes

Michael Busby,[†] Anders Gabrielsson,[†] Pavel Matousek,[‡] Michael Towrie,[‡] Angel J. Di Bilio,[§] Harry B. Gray,*[,§] and Antonín Vlček, Jr.*[,†]

Department of Chemistry and Centre for Materials Research, Queen Mary, University of London, Mile End Road, London E1 4NS, United Kingdom, Central Laser Facility, CCLRC Rutherford Appleton Laboratory, Chilton, Didcot, Oxfordshire OX11 0QX, United Kingdom, and Beckman Institute, California Institute of Technology, Pasadena, California 91125

Received December 20, 2003

The nature and dynamics of the lowest excited states of *fac*-[Re^{I}(L)(CO)$_3$(phen)]$^+$ and *fac*-[Re^{I}(L)(CO)$_3$(5-NO$_2$-phen)]$^+$ [L = Cl$^-$, 4-ethyl-pyridine (4-Etpy), imidazole (imH); phen = 1,10-phenanthroline] have been investigated by picosecond visible and IR transient absorption spectroscopy in aqueous (L = imH), acetonitrile (L = 4-Etpy, imH), and MeOH (L = imH) solutions. The phen complexes have long-lived Re^{I} → phen ^{3}MLCT excited states, characterized by CO stretching frequencies that are upshifted relative to their ground-state values and by widely split IR bands due to the out-of-phase A′(2) and A″ ν(CO) vibrations. The lowest excited states of the 5-NO$_2$-phen complexes also have ^{3}MLCT character; the larger upward ν(CO) shifts accord with much more extensive charge transfer from the Re^{I}(CO)$_3$ unit to 5-NO$_2$-phen in these states. Transient visible absorption spectra indicate that the excited electron is delocalized over the 5-NO$_2$-phen ligand, which acquires radical anionic character. Similarly, involvement of the -NO$_2$ group in the Franck–Condon MLCT transition is manifested by the presence of an enhanced ν(NO$_2$) band in the preresonance Raman spectrum of [Re^{I}(4-Etpy)(CO)$_3$(5-NO$_2$-phen)]$^+$. The Re^{I} → 5-NO$_2$-phen ^{3}MLCT excited states are very short-lived: 7.6, 170, and 43 ps for L = Cl$^-$, 4-Etpy, and imH, respectively, in CH$_3$CN solutions. The ^{3}MLCT excited state of [Re^{I}(imH)(CO)$_3$(5-NO$_2$-phen)]$^+$ is even shorter-lived in MeOH (15 ps) and H$_2$O (1.3 ps). In addition to ^{3}MLCT, excitation of [Re^{I}(imH)(CO)$_3$(5-NO$_2$-phen)]$^+$ populates a ^{3}LLCT (imH → 5-NO$_2$-phen) excited state. Most of the ^{3}LLCT population decays to the ground state (time constants of 19 (H$_2$O), 50 (MeOH), and 72 ps (CH$_3$CN)); in a small fraction, however, deprotonation of the imH$^{\bullet+}$ ligand occurs, producing a long-lived species, [Re^{I}(im$^{\bullet}$)(CO)$_3$(5-NO$_2$-phen)$^{\bullet-}$]$^+$.

Introduction

A Re^{I}-diimine, *fac*-[Re^{I}(imH)(CO)$_3$(phen)]$^+$, has been employed as a strong excited-state oxidant (+1.2 V vs SCE[1] in CH$_3$CN) and a moderate reductant (−0.7 V vs SCE in CH$_3$CN) in investigations of redox processes in Re^{I}-modified proteins.[2−7] As typical of most [Re^{I}(L)(CO)$_3$(polypyridine)]$^{n+}$ complexes,[8−14] the emissive excited state of [Re^{I}(imH)(CO)$_3$(phen)]$^+$ (τ = 120 ns in H$_2$O) has Re^{I} → phen ^{3}MLCT character (hereafter called ^{3}MLCT(phen)).[2] Since imidazole

* Authors to whom correspondence should be addressed. E-mail: hbgray@caltech.edu (H.B.G.); a.vlcek@qmul.ac.uk (A.V.).
[†] University of London.
[‡] Rutherford Appleton Laboratory.
[§] California Institute of Technology.

(1) Abbreviations: imH, imidazole; phen, 1,10-phenanthroline; SCE, saturated calomel electrode; py, pyridine; MLCT, metal-to-ligand charge transfer; LLCT, ligand-to-ligand charge transfer; IL, intraligand; triflate, trifluoromethanesulfonate; DMF, dimethyl formamide; ES-MS, electrospray mass spectrum; bpy, 2,2′-bipyridine.

(2) Connick, W. B.; Di Bilio, A. J.; Hill, M. G.; Winkler, J. R.; Gray, H. B. *Inorg. Chim. Acta* **1995**, *240*, 169−173.
(3) Winkler, J. R.; Di Bilio, A. J.; Farrow, N. A.; Richards, J. H.; Gray, H. B. *Pure Appl. Chem.* **1999**, *71*, 1753−1764.
(4) Di Bilio, A. J.; Crane, B. R.; Wehbi, W. A.; Kiser, C. N.; Abu-Omar, M. M.; Carlos, R. M.; Richards, J. H.; Winkler, J. R.; Gray, H. B. *J. Am. Chem. Soc.* **2001**, *123*, 3181−3182.
(5) Crane, B. R.; Di Bilio, A. J.; Winkler, J. R.; Gray, H. B. *J. Am. Chem. Soc.* **2001**, *123*, 11623−11631.
(6) Miller, J. E.; Grădinaru, C.; Crane, B. R.; Di Bilio, A. J.; Wehbi, W. A.; Un, S.; Winkler, J. R.; Gray, H. B. *J. Am. Chem. Soc.* **2003**, *125*, 14220−14221.
(7) Miller, J. E.; Di Bilio, A. J.; Wehbi, W. A.; Green, M. T.; Museth, A. K.; Richards, J. H.; Winkler, J. R.; Gray, H. B. *Biochim. Biophys. Acta* **2004**, *1655*, 59−63.

10.1021/ic035471b CCC: $27.50
Published on Web 07/10/2004

is a relatively strong electron donor, it is possible that imH → phen charge transfer (LLCT) accompanies MLCT excitation; indeed, with both a strong π electron acceptor (5-NO_2-phen) and an imidazole donor in the Re^I coordination sphere, the nature of the emissive state could change dramatically. Moreover, introduction of a nitro group on the phen ligand is expected to upshift the reduction potential of the complex, making it an even stronger excited-state oxidant.

We have investigated $[Re^I(imH)(CO)_3(phen)]^+$ and $[Re^I(imH)(CO)_3(5\text{-}NO_2\text{-}phen)]^+$ by picosecond time-resolved infrared (TRIR) and femtosecond visible transient absorption spectroscopy. For comparison, the complexes $[Re^I(4\text{-}Etpy)(CO)_3(phen)]^+$, $[Re^I(4\text{-}Etpy)(CO)_3(5\text{-}NO_2\text{-}phen)]^+$, and $[Re^I(Cl)(CO)_3(5\text{-}NO_2\text{-}phen)]$ were studied in CH_3CN solution, whose relaxation[15,16] is fast enough not to interfere with the intramolecular solute dynamics. In addition to the structural characterization of the lowest excited states of these Re^I−carbonyl−phenanthroline complexes, we have obtained information on their vibrational relaxation dynamics. Notably, we have found striking differences between the excited-state lifetimes and reactivities of the phen and 5-NO_2-phen complexes.

Experimental Section

fac-$[Re^I(imH)(CO)_3(phen)]_2SO_4\cdot 4H_2O$, *fac*-$[Re^I(4\text{-}Etpy)(CO)_3(phen)]$triflate, *fac*-$[Re^I(4\text{-}Etpy)(CO)_3(5\text{-}NO_2\text{-}phen)]$triflate, and *fac*-$[Re^I(Cl)(CO)_3(5\text{-}NO_2\text{-}phen)]$ were prepared by literature procedures.[2,9,17,18] *fac*-$[Re^I(4\text{-}Etpy)(CO)_3(NN)]PF_6$ (NN = phen, 5-NO_2-phen) was precipitated by addition of $(NH_4)PF_6$ to a methanol solution of the triflate salt. $[Re^I(imH)(CO)_3(5\text{-}NO_2\text{-}phen)]_2SO_4$ was prepared by reacting $[Re^I(L)(CO)_3(5\text{-}NO_2\text{-}phen)]$ (L = Cl^- or triflate) with aqueous 500 mM imidazole (adjusted to pH 7) at 80 °C for 8 h. The crude product was loaded into a column packed with Fast Flow S-Sepharose (Pharmacia) and eluted with aqueous $(NH_4)_2SO_4$. Orange $[Re^I(imH)(CO)_3(5\text{-}NO_2\text{-}phen)]_2SO_4$ precipitated from concentrated solutions. The product was redissolved in MeOH, the precipitated $(NH_4)_2SO_4$ was filtered off, and the solvent was removed (this step was repeated until all $(NH_4)_2SO_4$ was removed).

All spectroscopic measurements on *fac*-$[Re^I(4\text{-}Etpy)(CO)_3(NN)]PF_6$ (NN = phen, 5-NO_2-phen) were done in CH_3CN solution (these complexes are insoluble in water). Aqueous solutions of the imH complexes for TRIR measurements were prepared in D_2O containing 26.8 mM Na_2HPO_4 and 19.6 mM NaH_2PO_4 (pD ~ 7). H_2O was used instead of D_2O in transient visible absorption measurements. Solutions of $[Re^I(imH)(CO)_3(5\text{-}NO_2\text{-}phen)]_2SO_4$ in CH_3CN were prepared by stirring a suspension of the complex with a small excess of $(NH_4)PF_6$ for 10 min, followed by filtration.

$[Re^I(imH)(CO)_3(5\text{-}NO_2\text{-}phen)]_2SO_4\cdot 4H_2O$. ^{1}H NMR ($CD_3OD$, 300 MHz): 6.64 (1H, t, *J* 1.5), 6.92 (1H, t, *J* 1.2), 7.63 (1H, t, *J* 1.2), 8.27 (3H, m), 9.14 (1H, dd, ^1J 8.7 ^2J 1.5), 9.24 (1H, s), 9.43 (1H, dd, ^1J 8.7, ^2J 1.5), 9.77 (2H, m). ES-MS *m*/*z* 564.0 [M^+]. UV−visible (H_2O), 319 (sh), 352 nm (sh). Anal. Calcd for $C_{36}H_{28}N_{10}O_{18}Re_2S$: C, 33.49; H, 2.18; N, 10.8; S, 2.48. Found: C. 33.41; H, 2.37; N, 11.19; S, 2.64%.

$[Re^I(4\text{-}Etpy)(CO)_3(phen)]PF_6$. FT-IR ($CH_3CN$) ν_{CO} = 2035 (s), 1930 (br) cm^{-1}. ^{1}H NMR (CD_3CN, 270 MHz): 1.09 (3H, t, *J* 7.7, 4-Etpy CH_3), 2.53 (2H, q, *J* 7.4, 4-Etpy CH_2), 7.20 (2H, d, *J* 6.5, aromatic CH), 8.35 (4H, m, aromatic CH), 8.44 (2H, d, *J* 6.6, aromatic CH), 9.06 (2H, s, *J* 6.3, aromatic CH), 9.97 (2H, dd, *J* 8.2, aromatic CH). ES-MS *m*/*z* 558.2 [M^+]-PF_6.

$[Re^I(4\text{-}Etpy)(CO)_3(5\text{-}NO_2\text{-}phen)]PF_6$. FT-IR ($CH_3CN$) ν_{CO} = 2037(s), 1933 (br) cm^{-1}. ^{1}H NMR (CD_3CN, 270 MHz): 1.02 (3H, t, *J* 7.7, 4-Etpy CH_3), 2.49 (2H, q, *J* 7.2, 4-Etpy CH_2), 7.05 (2H, d, *J* 5.2, aromatic CH), 8.11 (2H, d, *J* 5.2, aromatic CH), 8.21 (2H, m, aromatic CH), 8.99 (1H, d, *J* 8.5, aromatic CH), 9.06 (1H, s, aromatic CH), 9.31 (1H, d, *J* 8.8, aromatic CH), 9.71 (2H, dd, *J* 4.9, aromatic CH). ^{13}C NMR (CD_3CN, 67.9 MHz): 13.07, 27.57, 124.12, 126.12, 127.15, 128.25, 128.43, 136.97, 142.24, 145.01, 145.99, 147.92, 148.39, 151.55, 155.85, 157.48, 158.27, 195.51 (CO). ES-MS *m*/*z* 603.2 [M^+]-PF_6.

Physical Methods. Crystals of $[Re^I(4\text{-}Etpy)(CO)_3(5\text{-}NO_2\text{-}phen)]PF_6$ were grown from methanol solution by slow solvent evaporation. X-ray diffraction data for $[Re^I(4\text{-}Etpy)(CO)_3(5\text{-}NO_2\text{-}phen)]PF_6$ were recorded in the $\omega/2\theta$ scan mode with a CAD4 diffractometer fitted with a low-temperature device. The structure was solved by standard heavy atom techniques and refined by least-squares fits on F^2.[19] Hydrogen atoms were calculated geometrically and refined with a riding model.

TRIR measurements were performed as described previously.[20−24] In short, samples were excited at 400 nm (150 fs fwhm) using frequency-doubled pulses from a Ti:sapphire laser and probed with IR pulses (150 fs fwhm) obtained by difference-frequency generation. The IR probe pulses covered a spectral range 150−200 cm^{-1} wide. Sample solutions flowed through a CaF_2 IR cell, which was rastering in two dimensions. Sample path lengths of 0.1 and 0.5−1 mm were used for D_2O and CH_3CN solutions, respectively. The spectral bands were fit with Lorentzian functions to determine their centers and shapes. Fittings of spectra and kinetics were performed using MicroCal Origin 7.0. Time-resolved visible difference spectra were measured using the apparatus at the Institute of Molecular Chemistry, University of Amsterdam.[25] With this setup, 393 nm pump pulses (130 fs fwhm) were generated by frequency doubling

(8) Geoffroy, G. L.; Wrighton, M. S. *Organometallic Photochemistry*; Academic Press: New York, 1979.
(9) Wrighton, M. S.; Morse, D. L. *J. Am. Chem. Soc.* **1974**, *96*, 998−1003.
(10) Luong, J. C.; Nadjo, L.; Wrighton, M. S. *J. Am. Chem. Soc.* **1978**, *100*, 5790−5795.
(11) Kalyanasundaram, K. *J. Chem. Soc. Faraday Trans.* **1986**, *82*, 2401−2415.
(12) Striplin, D. R.; Crosby, G. A. *Chem. Phys. Lett.* **1994**, *221*, 426−430.
(13) Striplin, D. R.; Crosby, G. A. *Coord. Chem. Rev.* **2001**, *211*, 163−175.
(14) Stufkens, D. J.; Vlček, A., Jr. *Coord. Chem. Rev.* **1998**, *177*, 127−179.
(15) Rosenthal, S. J.; Xie, X. L.; Du, M.; Fleming, G. R. *J. Chem. Phys.* **1991**, *95*, 4715−4718.
(16) Passino, S. A.; Nagasawa, Y.; Joo, T.; Fleming, G. R. *J. Phys. Chem. A* **1997**, *101*, 725−731.
(17) Fredericks, S. M.; Luong, J. C.; Wrighton, M. S. *J. Am. Chem. Soc.* **1979**, *101*, 7415−7417.
(18) Wallace, L.; Rillema, D. P. *Inorg. Chem.* **1993**, *32*, 3836−3843.
(19) Sheldrick, G. M. *SHELX-97*, *Program for Crystal Structure Determination and Refinement*; University of Göttingen: Germany, 1998.
(20) Matousek, P.; Towrie, M.; Stanley, A.; Parker, A. W. *Appl. Spectrosc.* **1999**, *53*, 1485−1489.
(21) Matousek, P.; Towrie, M.; Ma, C.; Kwok, W. M.; Phillips, D.; Toner, W. T.; Parker, A. W. *J. Raman Spectrosc.* **2001**, *32*, 983−988.
(22) Towrie, M.; Grills, D. C.; Dyer, J.; Weinstein, J. A.; Matousek, P.; Barton, R.; Bailey, P. D.; Subramaniam, N.; Kwok, W. M.; Ma, C. S.; Phillips, D.; Parker, A. W.; George, M. W. *Appl. Spectrosc.* **2003**, *57*, 367−380.
(23) Vlček, A., Jr.; Farrell, I. R.; Liard, D. J.; Matousek, P.; Towrie, M.; Parker, A. W.; Grills, D. C.; George, M. W. *J. Chem. Soc. Dalton Trans.* **2002**, 701−712.
(24) Liard, D. J.; Busby, M.; Farrel, I. R.; Matousek, P.; Towrie, M.; Vlček, A., Jr. *J. Phys. Chem. A* **2004**, *108*, 556−567.
(25) Vergeer, F. W.; Kleverlaan, C. J.; Stufkens, D. J. *Inorg. Chim. Acta* **2002**, *327*, 126−133.

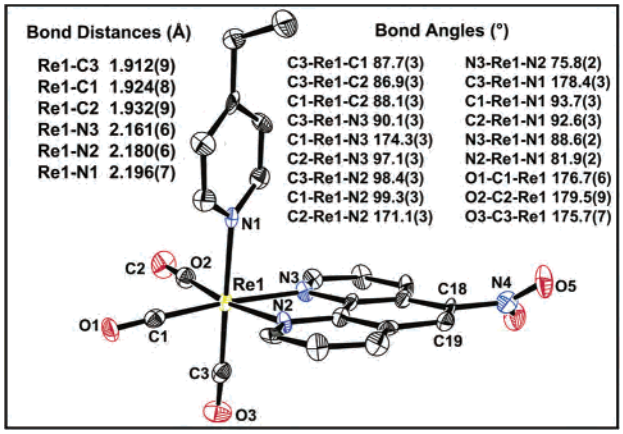

Figure 1. ORTEP diagram[29] for $[Re^{I}(4\text{-Etpy})(CO)_3(5\text{-}NO_2\text{-phen})]PF_6$ showing 40% probability ellipsoids (160 K). Hydrogens were omitted for clarity.

the output of a Ti:sapphire laser. White-light continuum probe pulses were generated by focusing the 800 nm fundamental on a sapphire plate.

The resonance Raman spectrum of $[Re^{I}(4\text{-Etpy})(CO)_3(5\text{-}NO_2\text{-phen})]^+$ was obtained using a UV Ar-ion laser (model Innova 90−5, Coherent) with an output of ∼50 mW at 457.9 nm. Sample solution flowed through a 2 mm quartz tube; the scattered light was collected at 90° from the excitation beam using a monochromator (SPEX Triplemate 187 Series) and dispersed across a CCD camera (model LN/CCD-1024, Princeton Instruments). Spectra were calibrated and solvent bands subtracted using CSMA CCD Spectrometric Multichannel Analysis Software V 2.4a (Princeton Instruments).

X-band EPR spectra were recorded with a Bruker EMX spectrometer equipped with a high sensitivity resonator (ER 4119HS). A built-in frequency counter provided accurate resonant frequency values. Variable temperature EPR measurements were performed with an ESR900 continuous-flow helium cryostat (Oxford Instruments). Measurements at 77 K were conducted using a finger Dewar. The 2−3 mM rhenium complex solutions were held in 4 mm (o.d.) quartz tubes. Samples under Ar were prepared by pump/fill cycles on a Schlenk line. The light source for steady-state photolysis was the focused beam from a 300 W Xe lamp (model PE300BF, Perkin-Elmer). Suitable filters were used to remove light below 350 nm. Data were acquired using a modulation amplitude of 2 G (100 kHz) and a microwave power of 5−50 μW.

Results

Structure of $[Re^{I}(4\text{-Etpy})(CO)_3(5\text{-}NO_2\text{-phen})]PF_6$. The structure of $[Re^{I}(4\text{-Etpy})(CO)_3(5\text{-}NO_2\text{-phen})]PF_6$ (Figure 1) is similar to those of other *fac*-$Re^{I}(CO)_3$−diimine complexes (see Supporting Information).[2,26]

The N3−Re1−N2 bite angle is characteristically small (75.8°). The molecular plane of the pyridine is approximately perpendicular to the phenanthroline plane and is rotated so that it intersects the angles between the N(phen) atoms and the equatorial carbonyls. The -NO_2 group is not coplanar with the phenanthroline. A 36.0° torsion angle was determined for the O5−N4−C18−C19 unit. The 5-NO_2-phenanthroline ligand differs in this respect from (planar) nitrobenzene.[27,28] Twisting of the -NO_2 group is caused by an attractive N−O···H interaction between 5-NO_2-phen ligands of neighboring molecules, for which an O(5)···H−C(12) distance of 2.485 Å was determined.

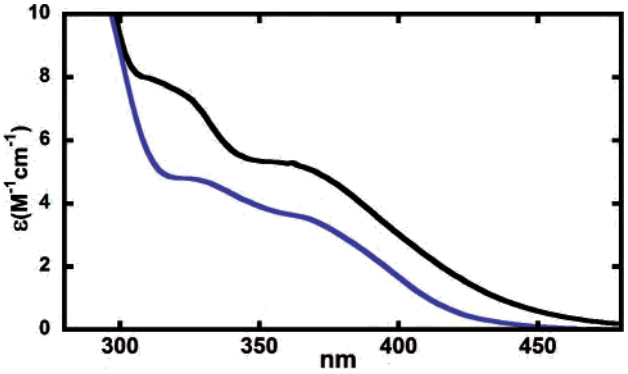

Figure 2. Absorption spectra measured in aqueous solution of $[Re^{I}(imH)(CO)_3(phen)]^+$ (blue trace) and $[Re^{I}(imH)(CO)_3(5\text{-}NO_2\text{-phen})]^+$ (black trace).

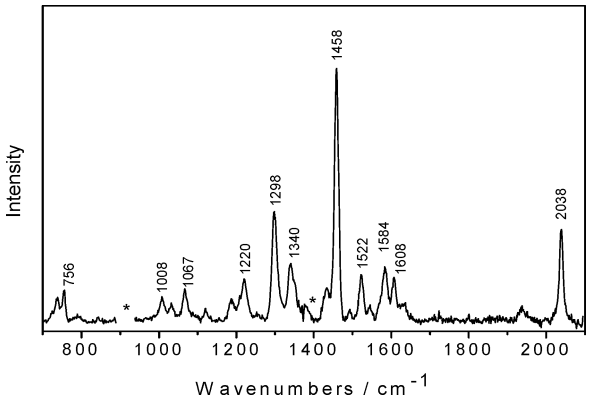

Figure 3. Preresonance Raman spectrum of $[Re^{I}(4\text{-Etpy})(CO)_3(5\text{-}NO_2\text{-phen})]^+$ in CH_3CN. The baseline was corrected for emission. Solvent signals were subtracted in the regions marked with an asterisk.

UV−Visible Absorption and Preresonance Raman Spectra. All the complexes show typical near-UV absorptions between 300 and 450 nm with an ϵ within the 4000−6000 $M^{-1}cm^{-1}$ range at ∼350 nm. The absorption spectra of the 5-NO_2-phen complexes are red-shifted by >10 nm relative to their phen counterparts (Figure 2).

These broad near-UV absorptions, which are characteristic of Re^{I}−carbonyl−polypyridine complexes, are attributable to MLCT and/or LLCT transitions.[9,13,14,17,30,31] More intense absorptions due to IL transitions occur at shorter wavelengths.

The preresonance Raman spectrum of $[Re^{I}(4\text{-Etpy})(CO)_3(5\text{-}NO_2\text{-phen})]^+$ (Figure 3) shows enhanced bands due to the in-phase A′(1) ν(CO) vibration of the $Re^{I}(CO)_3$ unit at 2038 cm^{-1}, high-frequency phen vibrations (1008, 1067, 1220, 1298(s), 1458(s) 1552, 1584, 1608 cm^{-1}) as seen in complexes such as $[Ru(phen)_3]^{2+}$ and $[W(CO)_4(phen)]$,[32−34]

(26) Busby, M.; Liard, D. J.; Motevalli, M.; Toms, H.; Vlček, A., Jr. *Inorg. Chim. Acta* **2004**, *357*, 167−176.
(27) Boese, R.; Blaser, D.; Nussbaumer, M.; Krygowski, T. M. *Struct. Chem.* **1992**, *3*, 363−368.
(28) Trotter, J. *Acta Crystallogr.* **1959**, *12*, 884−888.
(29) Farrugia, L. J. *J. Appl. Crystallogr.* **1997**, *30*, 565−565.
(30) Worl, L. A.; Duesing, R.; Chen, P. Y.; Della Ciana, L.; Meyer, T. J. *J. Chem. Soc. Dalton Trans.* **1991**, 849−858.
(31) Rossenaar, B. D.; Stufkens, D. J.; Vlček, A., Jr. *Inorg. Chem.* **1996**, *35*, 2902−2909.

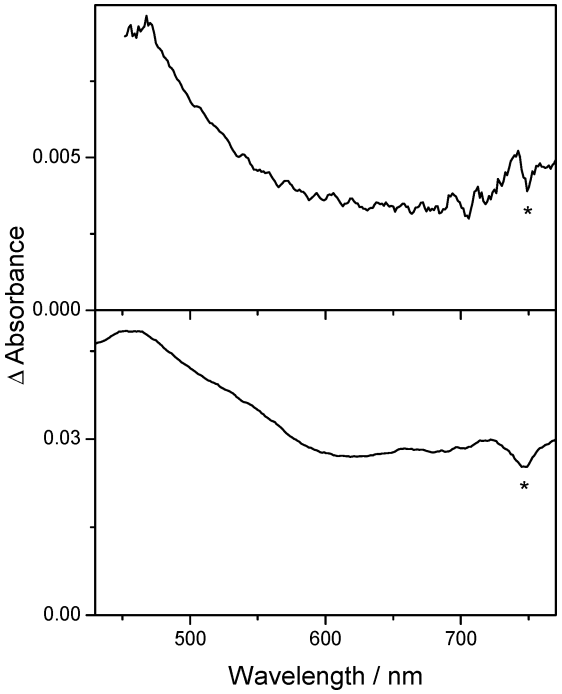

Figure 4. Difference spectra of $[Re^{I}(4\text{-Etpy})(CO)_3(phen)]^+$ in CH_3CN solution (top) and $[Re^{I}(imH)(CO)_3(phen)]^+$ in aqueous phosphate buffer (bottom) measured 2 ps after 393 nm laser excitation. No significant spectral changes were observed on a longer time scale (up to 1 ns). The spectra were smoothed by averaging every 10 adjacent points. Absorbance oscillations marked with an asterisk are due to an experimental artifact. (The transient difference spectra for these Re^{I} species are equivalent to absorption spectra as their ground-state absorptions in the visible are negligible.)

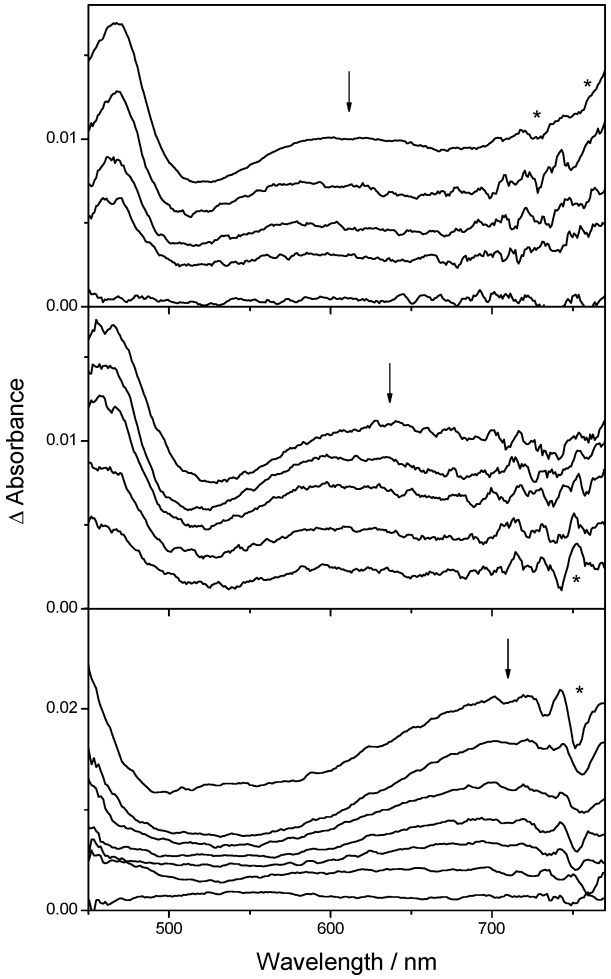

Figure 5. Difference spectra of $[Re^{I}(L)(CO)_3(5\text{-}NO_2\text{-phen})]^{n+}$ measured at selected time delays after 393 nm excitation. $[Re^{I}(Cl)(CO)_3(5\text{-}NO_2\text{-phen})](CH_3CN)$ at 2, 4, 8, 15, and 95 ps (top); $[Re^{I}(4\text{-Etpy})(CO)_3(5\text{-}NO_2\text{-phen})]^+$ (CH_3CN) at 2, 40, 80, 150, and 300 ps (middle); and $[Re^{I}(imH)(CO)_3(5\text{-}NO_2\text{-phen})]^+$ (aqueous phosphate buffer) at 1.5, 2, 2.5, 3, 4, 8, and 300 ps (bottom). The spectra evolved in the directions of the arrows. The spectra were smoothed by averaging every 10 adjacent points. Absorbance oscillations marked with an asterisk are due to an experimental artifact.

and a band at 1340 cm^{-1} that is characteristic of a $-NO_2$ group bonded to an aromatic ring.[35] This band, which is assigned to the symmetric $-NO_2$ stretch, is prominent in the resonance Raman spectrum of $[Ru(4\text{-}NO_2\text{-bpy})_3]^{2+}$, where it occurs at 1345 cm^{-1}.[36] This rR spectral pattern is typical of a localized MLCT transition.[31,37] Moreover, it indicates direct involvement of the nitro group in the Franck−Condon MLCT excitation.

Time-Resolved Visible Absorption Spectra. The spectra of $[Re^{I}(4\text{-Etpy})(CO)_3(phen)]^+$ (CH_3CN) and $[Re^{I}(imH)(CO)_3(phen)]^+$ (aqueous phosphate buffer) 2 ps after excitation at the low-energy edge of the MLCT band are shown in Figure 4. $[Re^{I}(4\text{-Etpy})(CO)_3(phen)]^+$ exhibits very weak excited-state absorption that increases in intensity at shorter wavelengths (Figure 4, top). An apparent maximum at ∼470 nm and a very weak band between 700 and 780 nm are seen. The transient spectrum of $[Re^{I}(imH)(CO)_3(phen)]^+$ is better developed, with a maximum at 460 nm and weaker bands at approximately 660 and 723 nm (Figure 4, bottom). For both complexes, these spectral features are attributed to the ^{3}MLCT(phen) excited state, based on a strong similarity with the nanosecond transient spectrum[11] of the typical ^{3}MLCT excited state of $[Re^{I}(Cl)(CO)_3(phen)]$, which shows a broad absorption at ∼480 nm. In agreement with long excited-state lifetimes (120 ns for the imH complex[2] and ∼1.6 μs expected for the 4-Etpy complex by analogy with $[Re^{I}(py)(CO)_3(phen)]^+$),[18] no absorbance decay was observed during the time interval studied (up to 1 ns).

Transient visible absorption spectra for $[Re^{I}(L)(CO)_3(5\text{-}NO_2\text{-phen})]^{n+}$ (L = Cl^-, 4-Etpy, and imH) are compared in Figure 5. All three complexes show a rapidly decaying broad absorption band covering most of the visible spectral region. The maximum of this absorption shifts to the red upon changing the ligand L in the order 590 (Cl^-), ∼605 (4-Etpy), and ∼695 nm (imH). The complexes also show a high-energy band with λ_{max} ∼467 nm (Cl^-) and ∼460 nm (4-Etpy); this band is shifted to the UV region for the imidazole complex. The excited-state visible spectral patterns of the 5-NO_2-phen complexes are similar to those observed for radical anions

(32) Schoonover, J. R.; Omberg, K. M.; Moss, J. A.; Bernhard, S.; Malueg, V. J.; Woodruff, W. H.; Meyer, T. J. *Inorg. Chem.* **1998**, *37*, 2585−2587.
(33) Chang, Y. J.; Xu, X.; Yabe, T.; Yu, S. C.; Anderson, D. R.; Orman, L. K.; Hopkins, J. B. *J. Phys. Chem.* **1990**, *94*, 729−736.
(34) Farrell, I. R.; Hartl, F.; Zalis, S.; Mahabiersing, T.; Vlček, A., Jr. *J. Chem. Soc. Dalton Trans.* **2000**, 4323−4331.
(35) Varsanyi, G. *Assignments for Vibrational Spectra of Seven Hundred Benzene Derivatives, Vol. 1*; New York, 1974.
(36) Basu, A.; Weiner, M. A.; Strekas, T. C.; Gafney, H. D. *Inorg. Chem.* **1982**, *21*, 1085−1092.
(37) Vlček, A., Jr. *Coord. Chem. Rev.* **2002**, *230*, 225−242.

Table 1. Ground- and Excited-State ν(CO) Frequencies (cm^{-1}) for $[Re^{I}((L)(CO)_3(phen)]^+$ and $[Re^{I}(L)(CO)_3(5\text{-}NO_2\text{-}phen)]^+$ (L = 4-Etpy, imH)[a]

	ground state			excited state[a]				
complex	A″	A′(2)	A′(1)	A″	A′(2)	A′(1)	$\Delta\nu$(A′(1))	τ (ps)
$[Re^{I}(4\text{-Etpy})(CO)_3(phen)]^+$	1930	1930	2035	1970	2013	2068	+33	>1 μs
$[Re^{I}(imH)(CO)_3(phen)]^+$	1925	1925	2032	1968	2013	2072	+40	120 ns
$[Re^{I}(4\text{-Etpy})(CO)_3(5\text{-}NO_2\text{-phen})]^+$	1931	1931	2037	1992	2037[b]	2104	+67	170
$[Re^{I}(imH)(CO)_3(5\text{-}NO_2\text{-phen})]^+$ (measured in D_2O, pH 7)	1928	1928	2033	*e*	*e*	2102[c]	+69[c]	1.3[c]
				~1901[d]	1974[d]	2010[d]	−23[d]	19[d]
$[Re^{I}(imH)(CO)_3(5\text{-}NO_2\text{-phen})]^+$ (measured in MeOH)	1927	1927	2033	~1994[c]	*e*	2103[c]	+70[c]	15[c]
				e	*e*	2013[d]	−20[d]	50[d]
$[Re^{I}(imH)(CO)_3(5\text{-}NO_2\text{-phen})]^+$ (measured in CH_3CN)	1926	1926	2033	1994[c]	~2048[c]	2105[c]	+72[c]	43[c]
				e	*e*	2020[d]	−13[d]	72[d]

[a] Spectral assignments are based on those given in ref 48. The observed early vibrational dynamics are summarized in ref 39. [b] Estimated value (the excited-state absorption overlaps the bleach). [c] ^{3}MLCT(5-NO_2-phen) excited state. [d] ^{3}LLCT excited state. [e] Band position cannot be determined because of spectral overlap.

of various nitro-aromatic compounds such as 1(2)-nitronaphthalene, nitrobenzene, and *o*-nitrotoluene,[38] which supports their assignment as ^{3}MLCT(5-NO_2-phen) or L → 5-NO_2-phen ^{3}LLCT excited states, formulated $^3[Re^{II}(L)(CO)_3(5\text{-}NO_2\text{-}phen^{\bullet-})]^{n+}$ and $^3[Re^{I}(L^{\bullet+})(CO)_3(5\text{-}NO_2\text{-}phen^{\bullet-})]^{n+}$, respectively.

The visible absorption bands slightly narrow and blue-shift during the first few picoseconds, presumably owing to vibrational cooling and solvation. The ^{3}MLCT excited states of the 5-NO_2-phen complexes are short-lived (Table 1). The lifetimes (in CH_3CN solution) determined from absorbance decays measured at several wavelengths across the spectrum are 7.6 ± 1.8 (L = Cl^-), 170 ± 20 (L = 4-Etpy), and 43 ± 8 ps (L = imH). $[Re^{I}(imH)(CO)_3(5\text{-}NO_2\text{-phen})]^+$ in aqueous solution shows more complicated behavior. The decay between 650 and 700 nm is biexponential with time constants of 1.3 ± 0.1 and 19 ± 2.4 ps, which contribute in an approximate ratio of 12:1. Decay is accompanied by a small blue shift of the 700 nm band. The broad absorption at ~690 nm is still present, albeit much weaker, in the spectra measured at time delays between 4 and 7 ps, which is well after the initial transient had decayed. This indicates either that the initial spectrum belongs to two different species, both containing 5-NO_2-phen$^{\bullet-}$, which decay with different time constants, or that the initially formed ^{3}MLCT(5-NO_2-phen) state decays simultaneously to the ground state and to another species, which still contains 5-NO_2-phen$^{\bullet-}$ and decays with a time constant of 19 ps. TRIR spectra reported below support the latter interpretation. A weak, very broad absorption at around 600 nm appears at ~8 ps and longer. This absorption weakens further and shifts to longer wavelengths at longer time delays, leaving a weak persistent feature between 500 and 600 nm.

Time-Resolved Infrared Spectroscopy. The picosecond TRIR difference spectra of $[Re^{I}(4\text{-Etpy})(CO)_3(phen)]^+$ and $[Re^{I}(imH)(CO)_3(phen)]^+$ show two negative bands originating from depletion of the ground-state population upon excitation and three positive excited-state bands that are shifted to higher frequencies relative to their respective ground-state positions (Figure 6). All these features appeared within the time resolution of the instrument. During the first 20 ps, the positive bands narrow and undergo a small dynamic shift to higher frequencies due to vibrational cooling and solvation (Figure 6).[39] The early dynamics are more

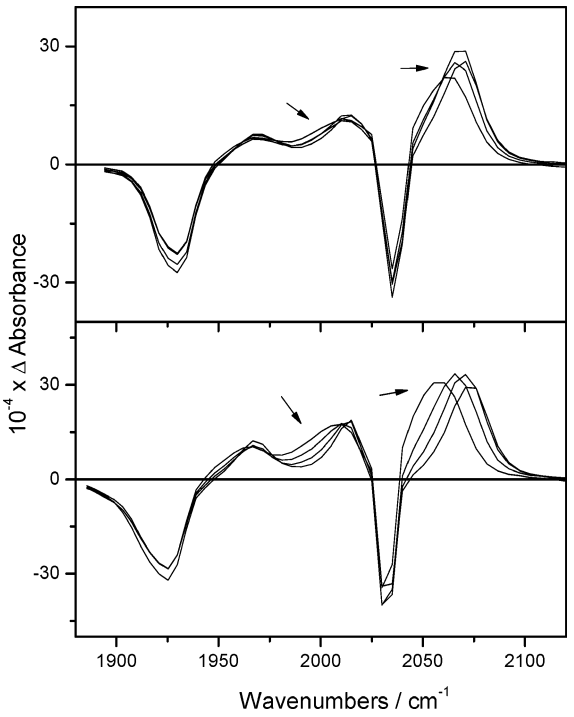

Figure 6. Difference TRIR spectra of $[Re^{I}(4\text{-Etpy})(CO)_3(phen)]^+$ in CH_3CN solution (top) and $[Re^{I}(imH)(CO)_3(phen)]^+$ in D_2O/phosphate (bottom) measured at 2, 4, 10, and 1000 ps after 400 nm excitation. The spectra evolved in the directions of the arrows. Experimental points are 4−5 cm^{-1} apart.

(38) Shida, T. *Physical Sciences Absorption Data 34. Electronic Absorption Spectra of Radical Ions*; Elsevier: Amsterdam, 1988.

(39) The following magnitudes and time constants were estimated for the initial (CO) dynamics: $[Re^{I}(4\text{-Etpy})(CO)_3(phen)]^+$, A′(1): shift +21.5 ± 2.5 cm^{-1}, 2.1 ± 0.2 ps, bandwidth decreases by ~43%, 1.4 ± 0.2 ps; A′(2): shift +3.2 ± 0.2 cm^{-1}, 8.7 ± 1.2 ps, bandwidth decreases by ~65%, 1.3 ± 0.2 ps. $[Re^{I}(4\text{-Etpy})(CO)_3(5\text{-}NO_2\text{-phen})]^+$, A′(1): shift +24.8 ± 3.3 cm^{-1}, 2.2 ± 0.3 ps (major), 16 ± 1.7 ps (minor). $[Re^{I}(imH)(CO)_3(phen)]^+$, A′(1): shift +25 ± 1.6 cm^{-1}, biexponential with major 2.5 ± 0.5 ps and minor ~27 ps components; narrowing by >50%, most of which occurs between 1.5 and 2 ps, followed by a small-amplitude 4.6 ps narrowing; A′(2): shift by +15 ± 1 cm^{-1}, biexponential with major 2.9 ± 0.3 ps and minor 20-40 ps components, narrowing by 33%, 6.7 ± 0.7 ps. $[Re^{I}(imH)(CO)_3(5\text{-}NO_2\text{-phen})]^+$ (CH_3CN), A′(1): shift +11.4 cm^{-1}, 8.4 ± 0.4 ps plus a faster component. $[Re^{I}(imH)(CO)_3(5\text{-}NO_2\text{-phen})]^+$ (MeOH), A′(1): shift 47.8 ± 1.3 cm^{-1}, 5.5 ± 0.3 ps. The excited-state frequencies in Table 1 were measured at longer time delays (typically 100 ps), with the exception of those for the excited state of $[Re^{I}(imH)(CO)_3(5\text{-}NO_2\text{-phen})]^+$ (D_2O).

prominent for $[Re^{I}(imH)(CO)_3(phen)]^+$. Notably, the bandwidth of the A′(1) vibrational feature shows an unusually fast initial narrowing between 2 and 4 ps. No spectral changes were observed on a longer time scale (up to 1 ns), in accord with their long excited-state lifetimes, suggesting that neither complex undergoes any fast photoreaction.

This TRIR spectral pattern is commonly observed for $Re^{I} \rightarrow$ diimine ^{3}MLCT excited states in *fac*-$[Re^{I}(L)(CO)_3(diimine)]^{n+}$ complexes, where the ν(CO) frequency increase signals a decrease in electron density on the $Re^{I}(CO)_3$ core upon excitation.[23,24,40−50] Splitting of the bands due to A″ and out-of-phase A′(2) vibrations that are essentially degenerate in the ground-state spectra of $[Re^{I}(L)(CO)_3(phen)]^+$ (L = 4-Etpy, imH) is another manifestation of $Re^{I} \rightarrow$ phen ^{3}MLCT excitation. The neutral N-donors phen, 4-Etpy, and imH have similar bonding properties toward Re^{I} in the ground state, keeping the local symmetry close to C_{3v}, in which the A″ and A′(2) vibrational modes coalesce into a single E mode. Reduction of the phen ligand in the excited state differentiates the equatorial and axial ligands, decreasing the local symmetry to C_s and splitting the E vibrational mode into A″ and A′(2).

Ground- and excited-state ν(CO) frequencies and assignments are set out in Table 1. The A′(1) band shifts upon excitation by +33 cm^{-1} for $[Re^{I}(4\text{-Etpy})(CO)_3(phen)]^+$ and +40 cm^{-1} for $[Re^{I}(imH)(CO)_3(phen)]^+$. These band shifts are comparable to those observed in the nanosecond time-domain for $[Re^{I}(Cl)(CO)_3(bpy)]$ (+40 cm^{-1}),[41] $[Re^{I}(4\text{-Etpy})(CO)_3(bpy)]^+$ (+39 cm^{-1}),[47,48] and $[Re^{I}(4\text{-Etpy})(CO)_3(4,4'\text{-}Me_2bpy)]^+$ (33−34 cm^{-1}).[24,47]

The TRIR spectra of $[Re^{I}(4\text{-Etpy})(CO)_3(5\text{-}NO_2\text{-phen})]^+$ (Figure 7, top) measured at time delays of 3 ps and longer show the same ^{3}MLCT excited-state pattern as those for the phen complexes. However, the upward shift relative to the ground state is much larger (67 cm^{-1}) for the A′(1) band, thereby indicating greater charge separation between $Re^{I}(CO)_3$ and 5-NO_2-phen in the ^{3}MLCT(5-NO_2-phen) excited state, with electron density delocalized over the $-NO_2$ group. (This shift is even larger than that reported[48] for $[Re^{I}(4\text{-Etpy})(CO)_3(4,4'\text{-}(COOEt)_2bpy)]^+$, +54 cm^{-1}.) The spectra measured at 1.5 and 2 ps are extremely broad, essentially

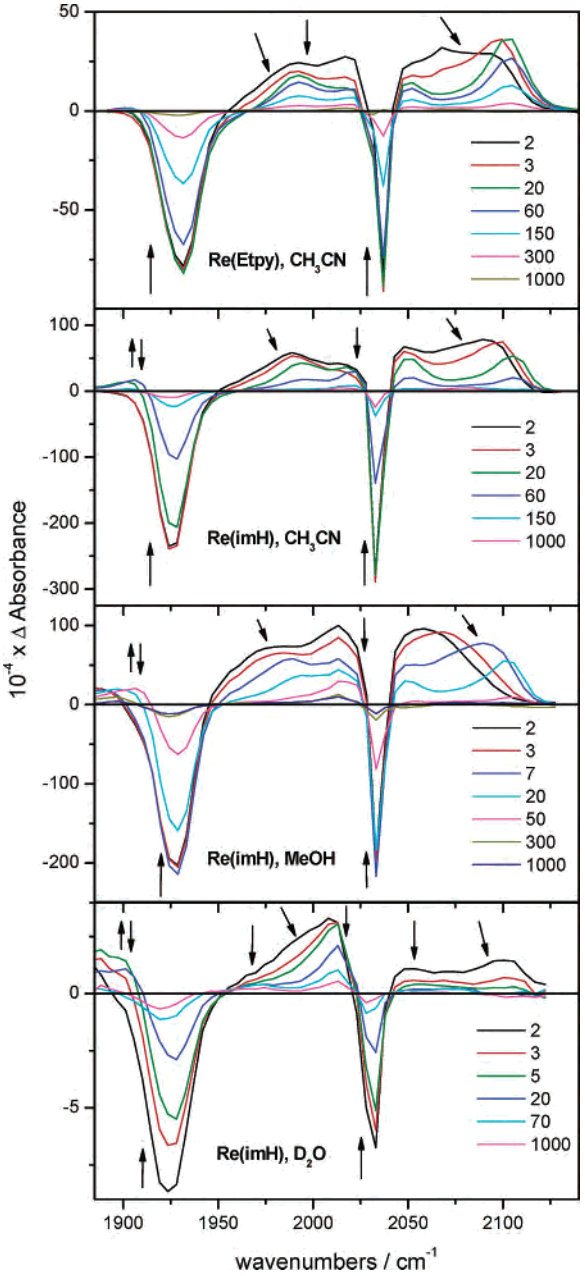

Figure 7. Difference TRIR spectra measured at selected time delays (ps) following 400 nm excitation: $[Re^{I}(4\text{-Etpy})(CO)_3(5\text{-}NO_2\text{-phen})]^+$ in CH_3CN (top) and $[Re^{I}(imH)(CO)_3(5\text{-}NO_2\text{-phen})]^+$ in CH_3CN, MeOH and D_2O/phosphate (bottom). The spectra evolved in the directions of the arrows. Points are 4−5 cm^{-1} apart.

covering the whole region examined. Individual ν(CO) bands develop only at ∼3 ps. Following the initial 3 ps period, all bands narrow and slightly blue shift. A 6 ps time constant was estimated for the ∼12 cm^{-1} upward shift of the A′(1) band. It follows that the initially formed ^{3}MLCT state is vibrationally very hot in low-frequency modes. The ^{3}MLCT state cools on two time scales, <3 and ∼6 ps. The spectra measured at 1.5−5 ps show an additional, rapidly decaying feature at 2068 cm^{-1} that is tentatively attributed to the "hot" $v = 1 \rightarrow 2$ A′(1) vibration. Following the early vibrational dynamics, the IR features decay in 162 ± 10 ps, in accord with the lifetime estimated from visible transient absorption decay.

(40) Glyn, P.; George, M. W.; Hodges, P. M.; Turner, J. J. *J. Chem. Soc. Chem. Commun.* **1989**, 1655−1657.
(41) George, M. W.; Johnson, F. P. A.; Westwell, J. R.; Hodges, P. M.; Turner, J. J. *J. Chem. Soc. Dalton Trans.* **1993**, 2977−2979.
(42) Gamelin, D. R.; George, M. W.; Glyn, P.; Grevels, F. W.; Johnson, F. P. A.; Klotzbucher, W.; Morrison, S. L.; Russell, G.; Schaffner, K.; Turner, J. J. *Inorg. Chem.* **1994**, *33*, 3246−3250.
(43) Asbury, J. B.; Wang, Y.; Lian, T. Q. *Bull. Chem. Soc. Jpn.* **2002**, *75*, 973−983.
(44) Bignozzi, C. A.; Schoonover, J. R.; Dyer, R. B. *Comments Inorg. Chem.* **1996**, *18*, 77−100.
(45) Schoonover, J. R.; Strouse, G. F.; Omberg, K. M.; Dyer, R. B. *Comments Inorg. Chem.* **1996**, *18*, 165−188.
(46) Schoonover, J. R.; Strouse, G. F. *Chem. Rev.* **1998**, *98*, 1335−1355.
(47) Dattelbaum, D. M.; Meyer, T. J. *J. Phys. Chem. A* **2002**, *106*, 4519−4524.
(48) Dattelbaum, D. M.; Omberg, K. M.; Schoonover, J. R.; Martin, R. L.; Meyer, T. J. *Inorg. Chem.* **2002**, *41*, 6071−6079.
(49) Liard, D. J.; Kleverlaan, C. J.; Vlček, A., Jr. *Inorg. Chem.* **2003**, *42*, 7995−8002.
(50) Liard, D. J.; Towrie, M.; Busby, M.; Matousek, P.; Vlček, A., Jr. *J. Phys. Chem. A* **2004**, *108*, 2363−2369.

The ultrafast spectroscopic behavior of $[Re^{I}(imH)(CO)_3(5\text{-}NO_2\text{-}phen)]^+$ is rather different from that of $[Re^{I}(imH)(CO)_3(phen)]^+$ and $[Re^{I}(4\text{-}Etpy)(CO)_3(5\text{-}NO_2\text{-}phen)]^+$. The TRIR spectra of $[Re^{I}(imH)(CO)_3(5\text{-}NO_2\text{-}phen)]^+$ (Figure 7, three bottom panels) show features due to the ^{3}MLCT excited state, which are the highly upshifted A′(1) band, the A′(2) band that strongly overlaps with the 2033 cm^{-1} bleach, and the A″ band at ~1994 cm^{-1}. All these features decay rapidly. ^{3}MLCT excited-state lifetimes of 15 ± 2 (MeOH) and 43 ± 8 ps (CH_3CN) were estimated from the decay of the A′(1) band. The ^{3}MLCT lifetime is much shorter in D_2O, where the corresponding spectral features are apparent only in the 1.5 (not shown) and 2 ps spectra at ~2102 cm^{-1}, essentially disappearing within the first 5 ps. In all three solvents, the fast decay of the A′(1) band is accompanied by a comparable decrease of the A′(2) absorption at 1990−1995 cm^{-1}. In addition to the ^{3}MLCT(5-NO_2-phen) features, the TRIR spectra show a second set of longer-lived bands: there is an intense maximum [2010 (D_2O), 2013 (MeOH), and 2020 cm^{-1} (CH_3CN)], which tails toward lower wavenumbers, and a feature at ~1901 cm^{-1}, which extends into the region of the 1928 cm^{-1} bleach. These IR features correspond to a state that contains a $Re^{I}(CO)_3$ core whose ν(CO) frequencies are lower than those of the parent ground-state complex. The time-resolved visible absorption spectra measured in H_2O at time delays of 4−8 ps indicate the presence of 5-NO_2-$phen^{\bullet-}$ (vide supra). Therefore, we assign the 2013 and 1901 cm^{-1} features to a ^{3}LLCT(imH → 5-NO_2-phen) state, $[Re^{I}(imH^{\bullet+})(CO)_3(5\text{-}NO_2\text{-}phen^{\bullet-})]^+$. Our assignment is further supported by the absence of a comparable intermediate in the decay of the ^{3}MLCT(5-NO_2-phen) excited state of $[Re^{I}(4\text{-}Etpy)(CO)_3(5\text{-}NO_2\text{-}phen)]$, whose 4-Etpy ligand is much more difficult to oxidize. The ^{3}LLCT state decays predominantly to the ground state (as manifested by parallel bleach recovery) and, in a minor parallel pathway, to another species that is characterized by bands at 2010, 1974 and ~1942 cm^{-1} in D_2O. Again, these bands indicate the presence of a $Re^{I}(CO)_3$ core and are tentatively attributed to a deprotonated imidazole radical species, $[Re^{I}(im^{\bullet})(CO)_3(5\text{-}NO_2\text{-}phen^{\bullet-})]$.[51] Similar low-yield irreversible photochemistry was seen also in MeOH, the product being characterized by a weak persistent feature at ~2013 cm^{-1}. The minor unidentified photoproduct observed at 1 ns in CH_3CN is characterized by very weak absorptions around 2080 and 2010−2020 cm^{-1}.

Analysis of the difference TRIR spectra measured in D_2O shows that the rapid decay of the ^{3}MLCT(5-NO_2-phen) absorptions (2102 and ~1990 cm^{-1}) and the following slower decay of the ^{3}LLCT state (2010 and ~1901 cm^{-1}) correspond to the 1.3 and 19 ps decays seen in the visible transient absorption experiments. In particular, a time constant of 1.7 ± 0.3 ps was estimated for the ^{3}MLCT(5-NO_2-phen) IR absorption in the 2098−2105 cm^{-1} range. The ^{3}LLCT band at 2010 cm^{-1} increases in the first 3−4 ps and then decays with a time constant of 23.0 ± 1.6 ps. (The early rise is difficult to analyze because of accompanying decay of the overlapping ^{3}MLCT absorption and bleach recovery.) Time profiles of the ^{3}LLCT absorptions at 1974 and 1901 cm^{-1} are difficult to analyze because of the weakness of the signal, interfering early rise, and an overlap (at 1901 cm^{-1}) with the bleach. Nevertheless, predominant 18.2 ± 1.6 and 18.8 ± 2.3 ps decay times were found at 1974 and 1901 cm^{-1}, respectively. (The latter kinetics were measured at 1888 cm^{-1}, as far as possible from the bleach. The initial apparent rise of the ~1901 cm^{-1} feature is mostly due to recovery of the overlapping negative bleach band.) The photoproduct absorptions at 2013, 1974, and ~1942 cm^{-1} decay very slowly, falling well beyond the time range investigated. Bleach recovery at 1928 cm^{-1} shows biexponential kinetics that are identical with those observed for the decay of both visible and IR transient absorptions. The recovery is characterized by time constants of 1.0 ± 0.2 and 18.9 ± 1.6 ps, which contribute approximately in a 3:1 ratio and leave a small residual long-lived bleach. Similar recovery (18.7 ± 1.3 ps) was found for the 2033 cm^{-1} bleach.

^{3}LLCT excited-state lifetimes of ~50 ps (MeOH) and 72 ps (CH_3CN) were estimated from the absorbance decay at 2013 and 2020 cm^{-1} and from the bleach-recovery kinetics. Spectra measured in CH_3CN clearly show an initial rise of the 2020 cm^{-1} band during the first 40 ps, presumably due to the ^{3}MLCT → ^{3}LLCT conversion. In MeOH, the ^{3}LLCT band at 2013 cm^{-1} appears fully developed at 2 ps and then decays. However, its early dynamics are obscured by overlap with the broad ^{3}MLCT absorption that undergoes a large dynamical shift to higher frequencies and simultaneously decays. Moreover, comparison of the intensities of respective TRIR features (Figure 7) demonstrates that the population of the ^{3}LLCT state relative to the ^{3}MLCT state is strongly solvent dependent, decreasing in the order $D_2O \gg$ MeOH > CH_3CN.

Discussion

The lowest allowed electronic transitions of $[Re^{I}(L)CO)_3(phen)]^+$ and $[Re^{I}(L)(CO)_3(5\text{-}NO_2\text{-}phen)]^+$ (L = imH, 4-Etpy) have Re^{I} → phen and Re^{I} → 5-NO_2-phen ^{1}MLCT character, as expected for Re^{I}−tricarbonyl−diimine complexes.[14] Direct involvement of the -NO_2 group in MLCT-(5-NO_2-phen) excitation is confirmed by the preresonance

(51) Formation of long-lived (≥1 s) paramagnetic photoproducts in solutions of $[Re^{I}(imH)(CO)_3(5\text{-}NO_2\text{-}phen)]^+$ was verified by conventional EPR spectroscopy. EPR measurements conducted on frozen aqueous solutions (irradiated while freezing)[4] of $[Re^{I}(imH)(CO)_3(5\text{-}NO_2\text{-}phen)]^+$ revealed signals 60−70 G wide featuring a sharp peak at $g \sim 2.006$ flanked by two smaller peaks (see Supporting Information). The intensity of the side peaks is pH- and solvent-dependent. Notably, similar spectra were observed from samples that were irradiated *after* being frozen. Much weaker signals were recorded after irradiation of rhenium samples dissolved in methanol, indicating that the aqueous medium greatly favors formation of the radical species. Addition of an electron acceptor, $[Co(NH_3)_5Cl]^{2+}$, did not change the EPR spectrum appreciably. However, a broad absorption at $g \sim 5.4$ in the EPR spectrum at 15 K signals that Co^{2+} was formed during photolysis. Simulations indicate that the EPR spectrum of the photogenerated radical is dominated by coupling of the unpaired electron to one nitrogen atom, $A_z(N) \sim 23$ G, $A_{x,y}(N) < 2$ G and an axial g tensor, $g_z \sim 2.004$, $g_{x,y} \sim 2.007$. One possibility is that the initially formed $[Re^{I}(imH)^{\bullet+}(CO)_3(5\text{-}NO_2\text{-}phen)^{\bullet-}]^+$ deprotonates in the aqueous medium; in a subsequent step, the biradical reacts with $[Co(NH_3)_5Cl]^{2+}$ to give $[Re^{I}(im^{\bullet})(CO)_3(5\text{-}NO_2\text{-}phen)]$. Clearly, the latter species also is formed in the absence of an electron acceptor, as similar EPR spectra are observed in the two cases.

Raman spectrum of $[Re^{I}(4\text{-Etpy})(CO)_3(5\text{-}NO_2\text{-phen})]^+$. For L = 4-Etpy, the lowest-lying excited states are the corresponding triplets, ^{3}MLCT(phen) and ^{3}MLCT(5-NO_2-phen). Charge separation is much larger in the ^{3}MLCT(5-NO_2-phen) states, where electron density is partly localized on the -NO_2 group. In the case of ^{3}MLCT(phen) excited states, charge separation seems to be somewhat larger for $[Re^{I}(imH)(CO)_3(phen)]^+$ in H_2O than for $[Re^{I}(4\text{-Etpy})(CO)_3(phen)]^+$ in CH_3CN, possibly attributable to the higher polarity of the aqueous medium. The initial excess energy deposited in the femtosecond-populated ^{3}MLCT states is rapidly distributed among low-frequency intramolecular, solute−solvent, and first solvation-shell modes that are anharmonically coupled[52] to ν(CO) vibrations.[53] This is evidenced[43,50,52−59] by the finding[39] that excited-state IR and visible absorption bands are initially broad and shifted to lower wavenumbers relative to their final positions determined at longer time-delays. Vibrational cooling[54−57] occurs during the first 10−20 ps and is manifested by a dynamical shift and narrowing of the ν(CO) bands (Figures 6 and 7). The rapid cooling measured in fast-relaxing[15,16] CH_3CN is similar to that observed for $[Re^{I}(Cl)(CO)_3(4,4'\text{-}R_2bpy)]$ (R = -COOH and -COOEt)[43] in DMF and MeOH. The band shift of $[Re^{I}(imH)(CO)_3(phen)]^+$ in D_2O solution is clearly biexponential, with a minor ∼18 ps component that is attributed to solvational dynamics. Similar behavior was observed for $[Re^{I}(Cl)(CO)_3(4,4'\text{-}R_2bpy)]$ in EtOH and longer chain alcohols.[43] The sharp decrease in the A′(1) bandwidth between 1 and 2 ps for $[Re^{I}(imH)(CO)_3(phen)]^+$ in D_2O is noteworthy.

The ^{3}MLCT(5-NO_2-phen) excited states are about 5 orders of magnitude shorter lived than the corresponding ^{3}MLCT(phen) states. The lack of room temperature emission for $[Ru^{II}(4\text{-}NO_2\text{-bpy})_3]^{2+}$, $[Re^{I}(Cl)(CO)_3(4,4'\text{-}(NO_2)_2\text{-bpy})]$, $[Re^{I}(4\text{-Etpy})(CO)_3(4,4'\text{-}(NO_2)_2\text{-bpy})]^+$, and $[Re^{I}(Cl)(CO)_3(5\text{-}NO_2\text{-phen})]$ suggests that short ^{3}MLCT excited-state lifetimes are typical of complexes with nitro groups on the diimine ligands.[9,36,60,61]

$[Re^{I}(imH)(CO)_3(5\text{-}NO_2\text{-phen})]^+$ exhibits more complicated behavior. Taken together, the time-resolved visible and IR measurements indicate the following mechanistic picture (Scheme 1): the ^{1}MLCT(5-NO_2-phen) Franck−Condon excited state is converted very rapidly both to ^{3}MLCT(5-NO_2-phen) and ^{3}LLCT excited states, which are formulated $^3[Re^{II}(imH)(CO)_3(5\text{-}NO_2\text{-phen}^{\bullet-})]^+$ and $^3[Re^{I}(imH^{\bullet+})(CO)_3(5\text{-}NO_2\text{-phen}^{\bullet-})]^+$, respectively. The ^{3}MLCT(5-NO_2-phen) state undergoes ultrafast decay to the ground state and to the ^{3}LLCT state. The ^{3}MLCT lifetime is solvent-dependent, increasing in the order 1.3 (H_2O), 15 (MeOH), and 43 ps (CH_3CN). The direct subpicosecond population of the ^{3}LLCT state from the Franck−Condon state is predominant in MeOH and D_2O, while slower ^{3}MLCT → ^{3}LLCT conversion prevails in CH_3CN (see Figure 7). The ^{3}LLCT state then returns to the ground state with a lifetime of 19 ps in D_2O and 50 ps in MeOH and, in a minor parallel pathway, reacts further to produce another species with a similar IR spectrum. It is suggested that this photochemical reaction involves deprotonation of the $imH^{\bullet+}$ ligand producing $[Re^{I}(im^{\bullet})(CO)_3(5\text{-}NO_2\text{-phen}^{\bullet-})]$ and/or homolysis of the Re−N($imH^{\bullet+}$) bond in the ^{3}LLCT state. The ^{3}LLCT state is somewhat longer lived in CH_3CN (72 ps).

Scheme 1. Excited-State Dynamics of $[Re^{I}(imH)(CO)_3(5\text{-}NO_2\text{-phen})]^+$; Lifetimes Measured in D_2O (pD ∼7)[a]

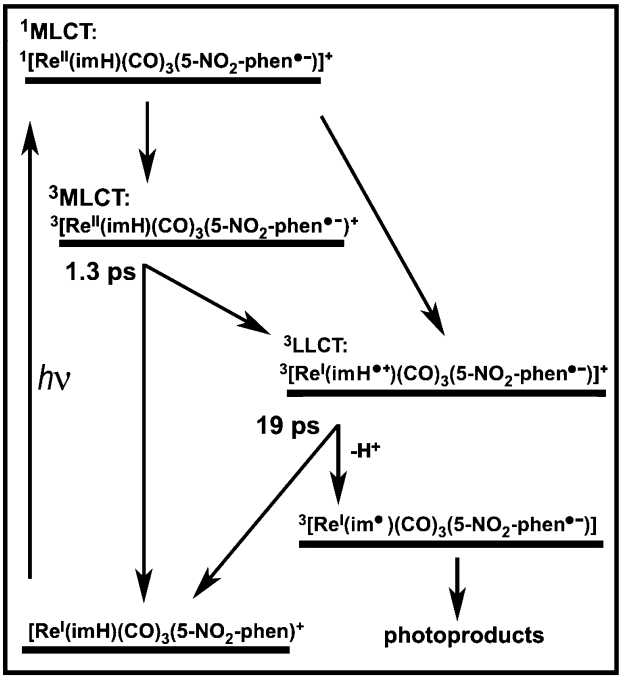

[a] Lifetimes in CH_3CN and MeOH are reported in the text and Table 1.

Concluding Remarks

We have shown that the water-soluble sensitizer $[Re^{I}(imH)(CO)_3(phen)]^+$ has a long-lived ^{3}MLCT excited state that can be formulated $^3[Re^{II}(imH)(CO)_3(phen^{\bullet-})]^+$. The extent of electron depopulation of the $Re^{I}(CO)_3$ core upon excitation is comparable to that observed in similar phenanthroline and bipyridine complexes. Imidazole is not involved in the excitation and remains intact at least up to 1 ns. Introduction of a nitro group at the 5-position of the phenanthroline ligand shortens the excited-state lifetime by almost 5 orders of magnitude, placing it in the picosecond time domain. Such short lifetimes prevent the use of NO_2-phen complexes as sensitizers in all but the fastest intramolecular reactions. We suggest that ultrafast oxidation of the axial imidazole ligand occurs in the case of electronically excited $[Re^{I}(imH)(CO)_3(5\text{-}NO_2\text{-phen})]^+$.

(52) Asher, S. A.; Murtaugh, J. *J. Am. Chem. Soc.* **1983**, *105*, 7244-7251.
(53) Dougherty, T. P.; Grubbs, W. T.; Heilweil, E. J. *J. Phys. Chem.* **1994**, *98*, 9396−9399.
(54) Hirata, Y.; Okada, T. *Chem. Phys. Lett.* **1991**, *187*, 203−207.
(55) Iwata, K.; Hamaguchi, H. *J. Mol. Liq.* **1995**, *65*−*6*, 417−420.
(56) Iwata, K.; Hamaguchi, H. *J. Phys. Chem. A* **1997**, *101*, 632−637.
(57) Hamaguchi, H.; Iwata, K. *Bull. Chem. Soc. Jpn.* **2002**, *75*, 883−897.
(58) Hamm, P.; Ohline, S. M.; Zinth, W. *J. Chem. Phys.* **1997**, *106*, 519−529.
(59) Nakabayashi, T.; Kamo, S.; Sakuragi, H.; Nishi, N. *J. Phys. Chem. A* **2001**, *105*, 8605−8614.
(60) Juris, A.; Campagna, S.; Bidd, I.; Lehn, J. M.; Ziessel, R. *Inorg. Chem.* **1988**, *27*, 4007−4011.
(61) Hino, J. K.; Della Ciana, L.; Dressick, W. J.; Sullivan, B. P. *Inorg. Chem.* **1992**, *31*, 1072−1080.

Acknowledgment. Majid Motevalli (QMUL) determined the crystal structure of $[Re^{I}(4\text{-Etpy})(CO)_3(5\text{-}NO_2\text{-phen})]PF_6$. We thank Mona Shahgholi, David Jenkins, and Larry Henling for helpful discussions. Time-resolved visible absorption spectra were measured with the kind help of Mikhail Zimin and M. Groeneveld at the Institute of Molecular Chemistry, University of Amsterdam, The Netherlands. I. P. Clark assisted with resonance Raman experiments at the LSF Nanosecond Laboratory at RAL. This work was supported by the EPSRC, COST Action D14 European collaboration program and NIH (DK19038).

Supporting Information Available: EPR spectra of irradiated frozen solutions of $[Re^{I}(imH)(CO)_3(5\text{-}NO_2\text{-phen})]_2SO_4$; crystal structure parameters for $[Re^{I}(4\text{-Etpy})(CO)_3(5\text{-}NO_2\text{-phen})]PF_6$ (PDF and CIF). This material is available free of charge via the Internet at http://pubs.acs.org. CCDC 227305 contains the supplementary crystallographic data for this paper. These data can be obtained free of charge via www.ccdc.cam.ac.uk/conts/retrieving.html (or from the CCDC, 12 Union Road, Cambridge CB2 1EZ, UK; fax: +44 1223 336033; e-mail: deposit@ccdc.cam.ac.uk).

IC035471B